

Clustering of soft colloids due to polymer additives

This article has been downloaded from IOPscience. Please scroll down to see the full text article.

2005 J. Phys.: Condens. Matter 17 S3363

(<http://iopscience.iop.org/0953-8984/17/45/023>)

View [the table of contents for this issue](#), or go to the [journal homepage](#) for more

Download details:

IP Address: 129.252.86.83

The article was downloaded on 28/05/2010 at 06:41

Please note that [terms and conditions apply](#).

Clustering of soft colloids due to polymer additives

C N Likos¹, C Mayer¹, E Stiakakis^{2,3} and G Petekidis²

¹ Institut für Theoretische Physik II, Heinrich-Heine-Universität Düsseldorf, Universitätsstraße 1, D-40225 Düsseldorf, Germany

² FORTH, Institute of Electronic Structure and Laser, GR-71110 Heraklion, Crete, Greece

³ Department of Chemistry, University of Crete, GR-71003 Heraklion, Crete, Greece

Received 16 September 2005

Published 28 October 2005

Online at stacks.iop.org/JPhysCM/17/S3363

Abstract

We examine theoretically the structural behaviour of dilute solutions of multiarm star polymers under the addition of smaller homopolymer chains. The approach is based on effective interactions, for which the star-polymer centres and the centres of mass of the linear chains are used as effective coordinates. We find that addition of linear chains first leads to a softening of the star-polymer repulsions and, at higher chain concentrations, to the formation of stable, multi-star clusters. We accompany the theoretical approach with dynamical light scattering measurements in real systems, finding agreement between theory and experiment. We rationalize our findings by deriving the chain-induced, one-component effective potential between stars, which features an attractive well followed by a repulsive barrier. We discuss the dependence of these characteristics on the size and concentration of the homopolymer additives and relate the present system to recent models that also display cluster formation.

Star-shaped polymers [1, 2] have emerged as a well characterized, tunable and highly versatile model colloidal system that displays very rich equilibrium and dynamical behaviour. The physical parameter that determines the softness of these macromolecular aggregates is the number f of polymer chains that are anchored on a common centre, also called the *functionality* of the star. Focusing on the mesoscopic length scales, the fluctuating monomers of the f chains in a concentrated star-polymer solution can be integrated out, leaving behind a collection of ‘effective point particles’ (the star centres) that interact by means of a monomer-mediated, soft effective repulsion [3]. The versatility of star polymers arises physically from the influence of the functionality f on the softness of this repulsion: it has been shown [4, 5] that it depends logarithmically on the star–star separation for overlapping distances, crossing over to an exponential decay for larger ones. The functionality influences both the overall strength of the repulsion, in the form of a $f^{3/2}$ -prefactor, and the decay length of the exponential tail, which scales as $\sigma f^{-1/2}$, with σ denoting the corona diameter of the star [5].

Whereas for sufficiently low functionalities, $f \leq f_c = 32$, the star–star repulsion is too weak to sustain stable crystals at arbitrary concentrations, for $f > f_c$ and above

the stars' overlap density stable bcc and fcc crystals are predicted to be the equilibrium structures, accompanied by re-entrant melting and formation of open crystal structures at even higher densities [6, 7]. The formation of ordered fcc and bcc crystals has recently found experimental confirmation for various star-like systems stemming from self-organized block copolymers [8–11]. Yet, for real star-polymer samples, the development of periodic structures is usually hindered by glass formation, aided by the inherent polydispersity of the solutions [12, 13]. A recent, mode-coupling analysis based on the effective interaction of [5] has shown that the vitrification of star polymers can be understood along the same lines as the dynamical arrest of a hard-sphere system, driven by the existence of a density-dependent, effective hard-sphere diameter between the stars [14]. Accordingly, the observed melting of the star-polymer glass upon addition of shorter homopolymer chains has been attributed to the ability of the additives to bring about a softening of the star–star repulsion and a concomitant reduction of the effective hard-sphere diameter between the same [15].

In this work, we keep our attention on star–chain mixtures but we turn our focus to the regime of low or intermediate concentrations of the stars, i.e., far from their overlap concentration and the associated crystallization or vitrification phenomena. We consider a mixture of star polymers with functionality f , termed species 1, with smaller linear chains, termed species 2. Following a coarse-graining procedure for both species, we describe the stars by their centres and the chains by their centres of mass. With r denoting the separation between any two such coordinates, the mesoscopic structure of the system can then be determined by three effective interaction potentials $v_{ij}(r)$, $i, j = 1, 2$, together with the physical characteristics of the system: the star functionality f and the chain-to-star size ratio $\delta < 1$, as well as the partial number densities $\rho_i = N_i/\Omega$, where N_i denotes the number of stars ($i = 1$) or chains ($i = 2$) enclosed in the macroscopic volume Ω . As we are dealing with polymers in athermal solvents throughout, the temperature appears in all effective interactions involved exclusively in the form of a prefactor $k_B T$ (with k_B being Boltzmann's constant), and therefore plays no role in the structure of the system.

For the three effective interactions $v_{ij}(r)$, we adopt the same expressions as used in a preceding study of the vitrification properties of star–chain mixtures by some of us [15]. The star–star interaction, $v_{11}(r)$, is given by the logarithmic Yukawa potential of [5], featuring a crossover from the logarithmic to the exponential form at the aforementioned length scale σ . Extensive computer simulations have established the relation $\sigma \cong 1.2R_g$ [16] between this length and the radius of gyration R_g of the stars. The chain–chain effective potential has been derived in the work of Louis *et al* [17, 18]: $v_{22}(r) = 1.87 k_B T \exp[-(r/\tau)^2]$, where $\tau = 1.13R_g^{\text{lin}}$ and R_g^{lin} is the linear chains' gyration radius. Finally, a heuristic form for the cross interaction, based on typical overlap energy estimates, has been adopted in [15], which reads as $v_{12}(r) = 1.387 k_B T (r/\xi)^{-12}$, with $\xi = (\sigma + 2\sigma/\sqrt{f} + R_g)/2$. The size asymmetry is expressed through the ratio $\delta \equiv \tau/\sigma < 1$.

In order to determine the pair structure of the mixture we have solved the *two-component* hypernetted chain (HNC) closure for given sets of physical parameters ($f, \delta; \rho_1, \rho_2$), deriving thereby the radial distribution functions $g_{ij}(r)$ and the structure factors $S_{ij}(q)$. In order to maintain contact with currently available experimental samples, we have considered three different values of the star functionality $f = 73, 122$, and 270 , as well as two different values of the size ratio $\delta = 0.3$ and 0.5 . The density ρ_1 was always kept within the dilute regime, $\rho_1 \sigma^3 \ll 1$, whereas ρ_2 was varied at will.

Selected results for the star–star structure factors $S_{11}(q)$ are shown in figure 1. Upon the addition of a small number of chains, the star system displays weakened correlations, as witnessed by the drop of the height of the main peak of $S_{11}(q)$ and the virtual disappearance of the second one. However, as ρ_2 further increases, a new feature shows up: the structure

factor develops a double-peak structure with two peaks that correspond to two independent length scales. Whereas a ‘particle peak’ shows up at $q_2\sigma \cong 6$, a ‘cluster peak’ appears at much smaller wavenumbers, $q_1\sigma \cong 2$, the position of which changes with chain density. In fact, as ρ_2 grows, the latter peak moves to lower q -values, indicating the growth of the cluster size (and the concomitant intercluster separation). Eventually, at sufficiently high chain densities, the peak moves towards $q = 0$ and a spinodal line, $S_{11}(q = 0) \rightarrow \infty$, is reached. The double-peak structure factor is strongly reminiscent of features present in model systems for which the development of clusters has been detected, both in experiment [19] and in theory [20–24]. We will return to a comparison between our system and some of these models at the end of this paper.

Comparing now the quantitative features of figures 1(a)–(c), we see that the occurrence of a double peak (and thus of the clusters) takes place at lower chain densities for $f = 73$ than for $f = 122$, at fixed size ratio $\delta = 0.3$. In fact, for star functionality $f = 270$, which we also examined, we did not find any clustering phenomena. Moreover, the interparticle distance within the clusters, r_m , which is given roughly as $r_m \cong 2\pi/q_2$, has a dependence both on f and on δ . Comparing figures 1(a) and (b) we see that, for fixed δ , the particles within the clusters come somewhat closer to each other as f increases. On the other hand, by comparing the position of q_2 between figures 1(b) and (c) we see that, for fixed f , an increase in δ leads to a concomitant increase of the particle separation within the clusters, witnessed by the significant shift of q_2 to the left. Otherwise, the position of q_2 is rather insensitive to the value of the density ρ_2 of the additives: clusters are formed and grow in size upon increasing ρ_2 but, otherwise, the particle–particle distance within a cluster is not influenced by the chain concentration.

Figure 2 shows the evolution of the radial distribution function $g_{11}(r)$ of the stars upon chain addition for the same parameter combination as in figure 1(b). The initial ‘softening’ of the star–star repulsion and the subsequent accumulation of stars are witnessed by the ‘leaking in’ of $g_{11}(r)$ and the development of an increasingly high peak at $r \gtrsim \sigma$, respectively. Note that, in agreement with the interpretation given above, the peak *position* is hardly affected by ρ_2 ; it corresponds to the length scale r_m introduced above. On the other hand, the integral below the peak, which gives the cluster size, does grow upon increase of ρ_2 .

We have also performed experiments employing mixtures of $f = 122$, regular 1,4-polybutadiene stars with homopolymer chains of size ratio $\delta = 0.4$. Dynamic light scattering experiments yielded the intermediate scattering function $C(q, t)$ which was analysed via an inverse Laplace transform, determining the characteristic relaxation times through the peak distribution of the same [25]. Such measurements allow for the independent determination of both the hydrodynamic radius and the radius of gyration of the dissolved objects for any given chain density. Indeed, the relaxation peaks resulting from the self-diffusion of the stars (slow) and the collective diffusion of the chains (fast) are well separated in time, allowing for the identification of two distinct relaxation processes in the system. Calling $\Gamma(q)$ the q -dependent inverse decay time associated with the stars, the self-diffusion coefficient D_{star} of the same was calculated as $D_{\text{star}} = \Gamma(q)/q^2$ and the Stokes–Einstein relation yielded the star hydrodynamic radius. On the other hand, the integrated intensity under the peak gives the *static* scattering intensity $I(q)$ from the stars, allowing then for a determination of the gyration radius R_g through a Guinier fit for the cluster-free case and by a Debye–Bueche fit in the clustered phase [26].

Both methods yielded identical results regarding the dependence of the radii on ρ_2 . In figure 3 we show the result for R_g . There is an initial shrinkage of the stars, caused by the osmotic pressure of the chains and lasting up to a concentration $c_{\text{lin}}/c_{\text{lin}}^* \cong 0.4$. Thereafter, a rapid increase of R_g was measured with growing chain concentration, pointing to the

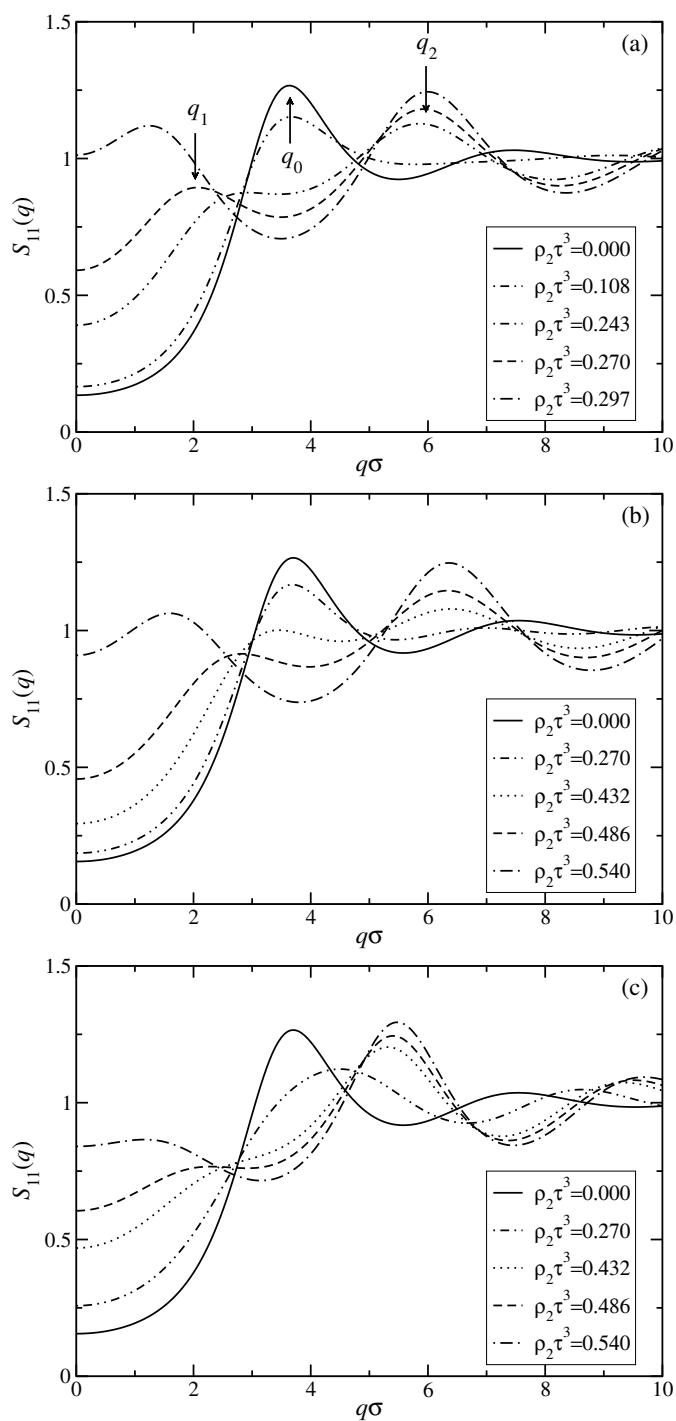


Figure 1. Star–star structure factors $S_{11}(q)$ for star polymers at density $\rho_1\sigma^3 = 0.1$ and chain densities $\rho_2\tau^3$ as indicated in the legends, for different star functionalities f and chain-to-star size ratios δ . (a) $f = 73$, $\delta = 0.3$; (b) $f = 122$, $\delta = 0.3$; (c) $f = 122$, $\delta = 0.5$. The arrows in (a) denote the cluster-peak position q_1 and the particle-peak position q_2 introduced in the text, whereas the peak position q_0 for the chain-free star solution is also marked for comparison.

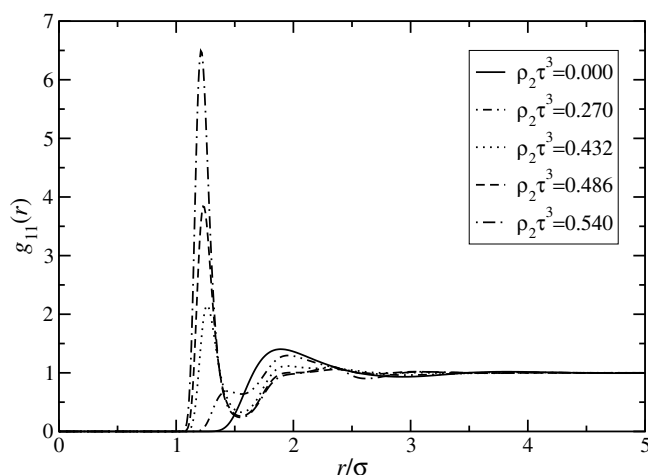


Figure 2. The star–star radial distribution function $g_{11}(r)$ at $\rho_1\sigma^3 = 0.1$ and chain densities $\rho_2\tau^3$ as indicated in the legends. Here $f = 122$ and $\delta = 0.3$.

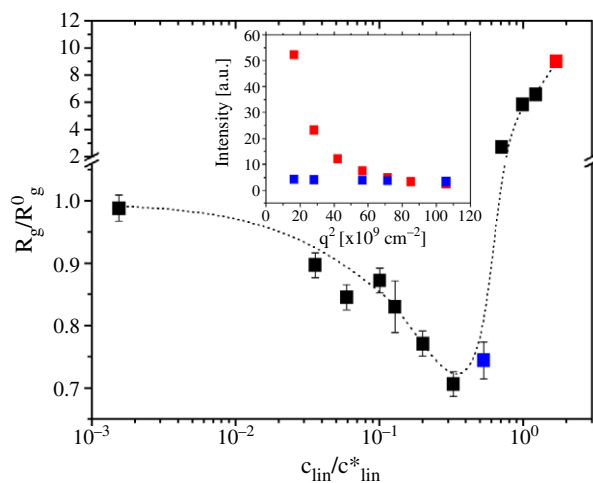


Figure 3. The ratio R_g/R_g^0 of the measured star radius of gyration over its value at zero chain concentration in a dilute star solution containing linear chains, plotted against the concentration of the latter. Here, c_{lin} denotes the weight fraction of linear chains with c_{lin}^* standing for the value of this quantity at the chains' overlap concentration. Inset: the measured scattering intensity at the last (upper symbols, red) and fifth from last (lower symbols, blue) points of the main plot. Notice the dramatic increase of the latter at low scattering wavevectors q at the red point, indicating the presence of clusters in the system.

(This figure is in colour only in the electronic version)

development of clusters with R_g as large as 10 times the value of an isolated star. After a period of several weeks, the clusters did not grow in size, suggesting their equilibrium nature.

The formation of clusters as well as the trends regarding their size and stability depending on f and δ can be rationalized through the concept of the effective star–star interaction *in the presence* of the chains, $V_{eff}(r; \rho_2)$. This quantity is derived from the stars' radial distribution function $g_{11}(r)$ through $V_{eff}(r; \rho_2) = -\lim_{\rho_1 \rightarrow 0} \ln g_{11}(r; \rho_1, \rho_2)$ and includes all the effects

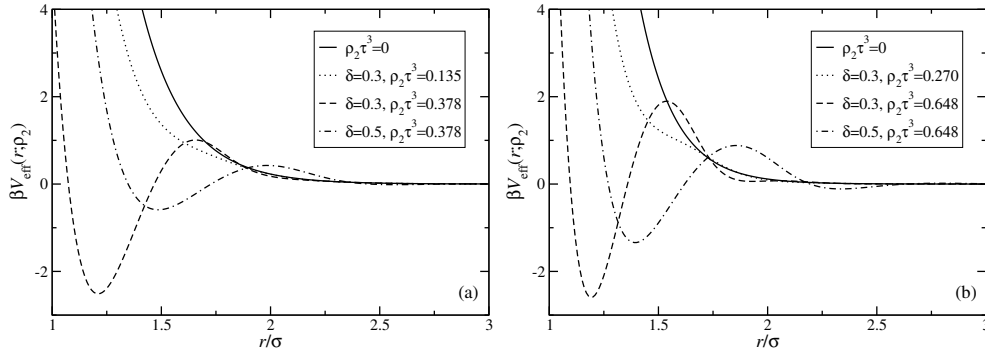


Figure 4. The chain-induced star–star effective interaction $V_{\text{eff}}(r; \rho_2)$ for various chain densities, as indicated in the legends. (a) $f = 73$; (b) $f = 122$. The size ratios δ are also shown in the legends.

from the chains through its dependence on the chain density ρ_2 . In the absence of chains, we have $V_{\text{eff}}(r; \rho_2 \rightarrow 0) = V_{11}(r)$. In figure 4 we show characteristic results for this quantity for different values of f , δ and ρ_2 . Whereas for small values of ρ_2 the effect of the chains is just a reduction of the repulsion strength of the interaction, upon sufficient increase of ρ_2 a ‘well-and-shoulder’ form of the effective interaction arises. The attractive well is a typical depletion effect and is caused by the osmotic pressure of the chains surrounding two stars that are sufficiently close to each other, so that polymer chains are excluded from the interstar space. The repulsive shoulder is a feature arising from the chain interactions and correlations, as the latter become crowded in the interstar region for larger interstar distances, a phenomenon also known from asymmetric hard sphere mixtures [27].

Cluster formation has been recently observed in protein solutions and charged colloid–polymer mixtures [19]; their stability was attributed to the presence of an effective potential with a short-range attraction and a long-range repulsion. The presence of *both* an attractive well and a repulsive shoulder is indispensable for the formation of finite, stable clusters. Indeed, in a number of recent works effective potentials of this kind have been employed in order to explain the emergence of mesoscopic structures (clusters or stripes) in soft matter. Sear and Gelbart worked with a hard-sphere potential, dressed by the superposition of two ‘Kac-tail’, long-range interactions, one attractive, causing the well, and one repulsive, giving rise to the shoulder [20]. Sciortino *et al* introduced an effective potential consisting of a superposition of a generalized $n-2n$ Lennard-Jones potential and a long-range Yukawa repulsion [21, 22], finding the formation of spherical or linear clusters, depending on parameter values. Liu *et al* investigated the structural properties of double Yukawa (attractive/repulsive) fluids, finding macrophase separation or cluster formation, depending on the relative strength of the attractive and repulsive parts [23], whereas Imperio and Reatto employed a model similar to that of [20] and discovered cluster and stripe formation in two dimensions [24]. The physics behind the cluster stability lies in the tendency of the attractive well to cause particle aggregates, whose size is thereafter limited by the repulsive barrier that prevents the growth of an infinite cluster. In this respect, the particle separation within the clusters, r_m , is set by the minimum in the effective potential $V_{\text{eff}}(r; \rho_2)$. This explains the observation that q_2 decreases (r_m grows) as δ increases; compare figure 4(b) with figures 1(a) and (b). Moreover, the fact that cluster formation is easier at fixed ρ_2 for smaller δ can be understood if one takes into account that, for given $\rho_2 \tau^3$, the number density of the small stars is larger for smaller δ , i.e., $\rho_2 \sigma^3 = \rho_2 \tau^3 / \delta^3$. Hence, the smaller- δ chains can bring about a higher osmotic pressure that leads to cluster

formation. Without the barrier, the system would be driven to phase separation without the occurrence of clusters, i.e., $S_{11}(q)$ would develop a peak at $q = 0$ and not at finite q -values [20]. Note, however, that the presence of clusters does *not* exclude macroscopic phase separation. Whereas one can choose the potential parameters in such a way that a binodal is completely eliminated or strongly suppressed [20–22], one can have situations in which a binodal line is preceded by a region of stability of finite clusters, as found by Liu *et al* in their study of the double-Yukawa system [23]. Here, we find a similar scenario, in which cluster formation is followed by indications of a macroscopic phase separation, i.e., star–chain demixing, witnessed by the drifting of the cluster peak towards $q = 0$ as ρ_2 is increased. Due to lack of experimental samples, the chain concentration could not be increased beyond the values quoted here. On the basis of the theoretical analysis, a macrophase separation is expected upon further increase of ρ_2 . The investigation of this question, both theoretically and experimentally, will be the subject of future work, along with related questions on the influence of the added chains on the gelation and vitrification properties of the stars.

Acknowledgments

The authors wish to thank Dimitris Vlassopoulos (FORTH) for helpful discussions and acknowledge the contributions of Hermis Iatrou and Nikos Hadjichristidis (Athens) and Jacques Roovers (Ottawa) in synthesizing the multiarm star polymers. CM thanks the Düsseldorf Entrepreneurs Foundation for a PhD Fellowship. This work has been supported by the EU, through grants RTN-2000-00017 and HPMF-CT-2002-01959 as well as through the Network of Excellence ‘Softcomp’.

References

- [1] Grest G S *et al* 1996 *Adv. Chem. Phys.* **94** 67
- [2] Daoud M and Cotton J P 1982 *J. Physique* **43** 531
- [3] Likos C N 2001 *Phys. Rep.* **348** 267
- [4] Witten T A and Pincus P A 1986 *Macromolecules* **19** 2509
- [5] Likos C N *et al* 1998 *Phys. Rev. Lett.* **80** 4450
- [6] Watzlawek M *et al* 1999 *Phys. Rev. Lett.* **82** 5289
- [7] Witten T A *et al* 1986 *Europhys. Lett.* **2** 137
- [8] Bang J *et al* 2002 *Phys. Rev. Lett.* **89** 215505
- [9] Lodge T P *et al* 2004 *Phys. Rev. Lett.* **92** 145501
- [10] Bang J and Lodge T P 2004 *Phys. Rev. Lett.* **93** 245701
- [11] Laurati M *et al* 2005 *Phys. Rev. Lett.* **94** 195504
- [12] Vlassopoulos D *et al* 2001 *J. Phys.: Condens. Matter* **13** R855
- [13] Kapnistos M *et al* 2000 *Phys. Rev. Lett.* **85** 4072
- [14] Foffi G *et al* 2003 *Phys. Rev. Lett.* **90** 238301
- [15] Stiakakis E *et al* 2002 *Phys. Rev. Lett.* **89** 208302
- [16] Jusufi A *et al* 1999 *Macromolecules* **32** 4470
- [17] Louis A A *et al* 2000 *Phys. Rev. E* **62** 7961
- [18] Louis A A *et al* 2000 *Phys. Rev. Lett.* **85** 2522
- [19] Stradner A *et al* 2004 *Nature* **432** 492
- [20] Sear R P and Gelbart W M 1999 *J. Chem. Phys.* **110** 4582
- [21] Sciortino F *et al* 2004 *Phys. Rev. Lett.* **93** 055701
- [22] Mossa S *et al* 2004 *Langmuir* **20** 10756
- [23] Liu Y *et al* 2005 *J. Chem. Phys.* **122** 044507
- [24] Imperio A and Reatto L 2004 *J. Phys.: Condens. Matter* **16** S3769
- [25] Provencher S W 1982 *Comput. Phys. Commun.* **27** 213
- [26] Higgins J A and Benoît H C 1986 *Polymers and Neutron Scattering* (Oxford: Clarendon)
- [27] Götzelmann B *et al* 1998 *Phys. Rev. E* **57** 6785